

A New Laboratory Method for Evaluation of Sulfate Scaling Parameters From Pressure Measurements

T. Carageorgos, University of Adelaide; M. Maroffi, SPE, State North Fluminense University of Rio de Janeiro; and P. Bedrikovetsky, SPE, University of Adelaide

Summary

Sulfate scaling in offshore waterflood projects, in which sulfate from the injected seawater (SW) reacts with metals from the formation water (FW), forming salt deposit that reduces permeability and well productivity, is a well known phenomenon. Its reliable prediction is based on mathematical models with well-known parameters.

Previous research presents methods for laboratory determination of model coefficients using breakthrough concentration during coreflooding. The concentration measurements are complex and cumbersome, while the pressure measurements are simple and require standard laboratory equipment. In the present work, a new laboratory method is developed for determination of the model coefficients from pressure measurements. Several laboratory corefloods have been performed. The tests show that the proposed method is more precise for artificial cores than for the natural reservoir cores. Further development of the method is required to determine parameters of formation damage caused by sulfate scaling for reservoir core samples.

Introduction

Ba/SrSO₄ scaling is a chronic disaster in waterflood projects with incompatible injected water and FW. Barium sulfate and related scale occurrence is considered to be a serious potential problem that causes formation damage near the production-well zone (Mackay et al. 2002; Mackay and Graham 2002; Mackay 2002; Gomes et al. 2002; Rosario and Bezerra 2001). This phenomenon is attributed to precipitation of barium/strontium sulfate from the mixture of both waters and the consequent permeability reduction resulting in well-productivity losses. The chemical incompatibility between the injected SW, which is high in sulfate ions, and the FW, which originally contains high concentrations of barium, calcium, and/or strontium ions, may result in disastrous well-productivity decline with consequent economic damage to the waterflood project (Oddo and Tomson 1994; Civan 2007).

A reliable model capable of predicting such scaling problems may be helpful in planning a waterflood scheme. It may also aid in selection of an effective scale-prevention technique through the prediction of scaling tendency, type, and potential severity. A reliable predictive model must use well-known values of the model coefficients.

The mathematical model for sulfate scaling contains two phenomenological parameters: (1) the kinetics coefficient from the active-mass law of chemical reaction showing how fast the reaction goes, and (2) the formation-damage coefficient reflecting the permeability decrease because of sulfate salt deposit (Araque-Martinez and Lake 1999, 2001; Delshad and Pope 2003; Kechagia et al. 2002; Philips 1991; Rocha et al. 2001; Yortsos 1990; Woods and Parker 2003).

Both coefficients are phenomenological parameters that depend on rock-surface mineralogy, pore-space structure, temperature, and

brine ionic strength. Therefore, they cannot be calculated theoretically for natural reservoirs and must be determined from laboratory corefloods by solving the corresponding inverse problem.

Reagent and deposition concentration profiles during reactive flows are nonuniform. So, the sulfate damage parameters cannot be calculated directly from laboratory measurements. Therefore, they must be determined from laboratory coreflood data using solutions to inverse problems.

The quasisteady-state commingled corefloods by FW and SW were performed by numerous authors (Lopes 2002; Read and Ringen 1982; Todd and Yuan 1992; Wat et al. 1992). Simple analytical models for quasisteady-state reactive flow allow for simple solutions of inverse problems to determine the model parameters from the test data.

The kinetics coefficient can be calculated from breakthrough concentration in quasisteady-state coreflood with commingled injection of SW and FW; then, the formation-damage coefficient can be determined from pressure-drop increase during coreflooding (Bedrikovetsky et al. 2004).

The pressure-drop measurements are simple and robust, while the breakthrough concentration determination is a cumbersome laboratory procedure. Therefore, often, concentration data are unavailable (Read and Ringen 1982).

The method for characterization of the scaling-damage system from pressure measurements (Bedrikovetsky et al. 2007) treats data from two corefloods performed with different ratios of FW to injected water. On the basis of an analytical model for commingled coreflood by SW and FW, the increase in pressure drop on the core during two corefloods allows determining the two scaling-damage parameters. The experimental data for three different corefloodings, performed to validate the method, exhibit excellent agreement.

The above-mentioned method uses the results of coreflooding in two separate artificial cores with identical properties. Applying the method to real reservoir cores is restricted by nonexistence of identical natural cores. The current paper reports the results of commingled injection of incompatible waters into different natural Berea cores. If compared with the results from identical artificial cores, the method stability in natural cores is lower.

In this paper another method to characterize the sulfate-scaling system from coreflood with pressure measurements at the same core is also proposed. Using the same core is the particularity of the proposed method. Two sequential commingled injections of FW and of SW are performed in the same core with different ratios of FW to injected water. Two sulfate-scaling-damage coefficients are determined from two different slopes of skin-factor increase during two injections. The sequence of two commingled waterfloodings was performed for a natural reservoir core, and the method proposed was applied to treat the results. The obtained coefficient values are in a reasonable agreement with those obtained from breakthrough concentration measured during the tests.

The structure of the paper is as follows. First, sulfate scaling in cores and in reservoirs is described, and the problem of scaling-damage characterization from pressure measurements during laboratory coreflooding is formulated. Then we follow the mathematical model for reactive transport of incompatible waters accounting for permeability damage and analytical model for quasisteady-state coreflood with simultaneous injection of SW and FW. The detailed

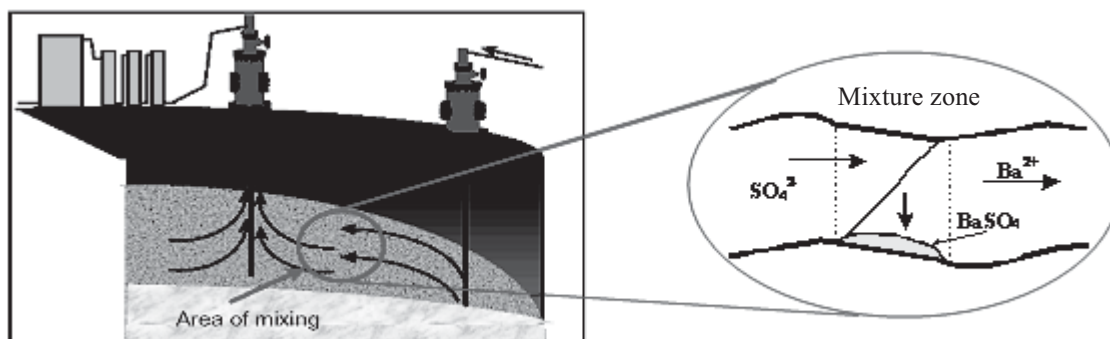


Fig. 1—Precipitation of barium sulfate in the mixing zone in stream tube during the displacement of FW by injection water.

derivations are presented in Appendixes A and B. An analytical-model-based explicit formula for rise of the pressure drop on the core during coreflooding allows deriving one transcendental equation to determine the kinetics coefficient. In the next section, the formation-damage coefficient is calculated explicitly from the pressure-drop rise. Then, the laboratory data for artificial cores are treated, and the values of both scaling-damage parameters for a series of three laboratory tests are presented. Equality of the parameter values, as obtained from three similar artificial cores, validates the proposed method. Afterward, we present data of the coreflooding with three different SW/FW ratios using natural reservoir cores. At the end, we describe the proposed method of coreflooding of a single core and the data treatment of the laboratory tests.

Formulation of the Problem

We discuss the formation damage caused by barium sulfate precipitation, which is one of the main physical mechanisms for production-well productivity decline. Usually SW, which contains SO_4^{2-} anions, is injected in offshore operations. If the FW contains Ba^{2+} cations, mixing of injected water and FW may cause BaSO_4 deposition (Fig. 1):



Similar reactions take place between sulfate anions and cations of strontium, calcium, and other metals (Oddo and Tomson 1994; Bethke 1996).

Sulfate salt deposition takes place in the mixing zone of the two waters. During waterflooding, the mixing zone moves continuously from injector to producer along the stream lines (see Fig. 1). The deposit accumulation in any reservoir pattern takes place during the short time, when the mixture zone passes the pattern. The zoom in the figure shows the mixing zone between the advancing injected water and displaced formation water, where barium sulfate precipitation occurs. This kind of deposit occupies a negligible fraction of pore space and does not cause significant permeability damage (Sorbie and Mackay 2000; Mackay 2002).

Some sulfate salt precipitation occurs also on the boundaries between the layers with contrasting permeabilities. In the case of vertical wells, the boundaries are mostly horizontal and do not cross streamlines. Therefore, this kind of in situ precipitation in the reservoir also does not cause significant formation damage (Sorbie and Mackay 2000).

Continuous mixing of injected water and FW takes place near the production wells, where simultaneous production of injected water by means of highly permeable layers and of produced water by means of low-permeability layers also occurs. Injected water and FW, arriving by different-length streamlines, also mix near the producers. The high flow velocity near the production wells intensifies the mixing and, consequently, the precipitation. Precipitation results in deposit accumulation near production wells, which causes the productivity to decline (Mackay 2002; Sorbie and Mackay 2000).

Reliable prediction of sulfate-scaling productivity decline is based on mathematical modeling with well-known values of the model coefficients. One way around the problem of the model-coefficient determination is solving the inverse problem for laboratory corefloods with a commingled injection of SW and FW (Bedrikovetsky et al. 2007).

Fig. 2 shows the laboratory procedure and setup for commingled corefloods (Yuang and Todd 1991; Todd and Yuan 1992; Wat et al. 1992). Two pumps inject both waters into the core. Constant pressure is maintained at the core effluent, and the pressure transducer measures the pressure drop on the core $\Delta p(t)$. The core is confined up to the overburden pressure; the confinement pressure is measured by manometer. The flow velocity U is measured by flowmeter. Barium concentration is measured in the injected water and also in the effluent samples.

The core with possible salt-deposition profile is shown in Fig. 3. Reagent concentrations decrease along the core, caused by chemical reaction. Therefore, the salt-deposition profile also declines along the core. The measured data used to characterize the sulfate-scaling system are the histories of the effluent concentration and of the “reciprocal injectivity index” $\Delta p/U$.

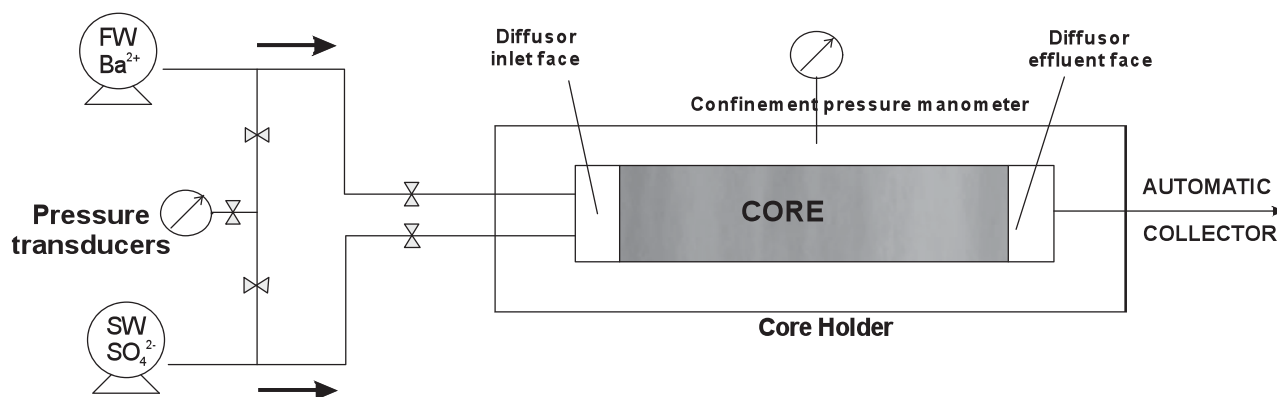


Fig. 2—Experimental setup for commingled injection of incompatible waters.

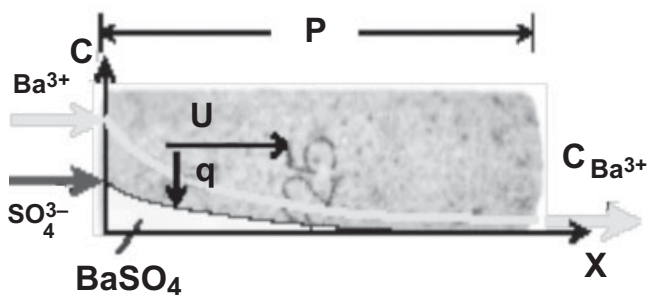


Fig. 3—Photo of the core and schematic of the quasisteady-state test with commingled injection of SW and FW.

During the tests, performed by Read and Ringen (1982) on commingled injection of FW and SW with the different FW to SW ratios, the flow rate and pressure drop in each flooding have been measured. The results are presented in Fig. 4. Four curves correspond to different FW/SW ratios.

Curve 1 corresponds to FW/SW=9:1. The injected concentrations for barium in FW and for sulfate in SW are 210 and 2300 ppm, respectively. The sulfate concentration exceeds that of barium 11 times. Therefore, the ratio of injected concentrations of barium to sulfate is 0.82 (i.e., the injected concentrations have the same order of magnitude). For the second curve that corresponds to FW/SW=3:1, the injected concentration ratio of barium to sulfate is 0.27 (i.e., sulfate concentration exceeds that of barium). The stoichiometric coefficients for Reaction 1 are equal to unity. So, the reaction rate in the second case (in which one reagent concentration highly exceeds the other one's concentration) is lower than that for the first case, in which reagent concentrations are almost equal. Therefore, Curve 1 in Fig. 4 is located above Curve 2. The barium/sulfate concentration ratio decreases further in Cases 3 and 4, resulting in decrease of the formation damage.

The tests have been performed for artificial cores with equal properties, for the same temperature and using the same SW and FW. So, the chemical-reaction and deposition conditions in the tests are the same. The results of corefloods with different FW/SW ratios are independent sources of information. Therefore, it is reasonable to pose the inverse problem for determination of the model coefficients from the data of different tests. It is expected that this inverse problem is well posed (Tikhonov and Arsenin 1977).

Characterization of the sulfate-scaling-damage system from laboratory data (Fig. 4) presented later in the text is based on inverse problems for a mathematical model of reactive flow in rocks (Alvarez et al. 2006a, 2006b).

Direct and Inverse Problems for Sulfate-Scaling Formation Damage

Let us describe the mathematical model for 1D reactive flow in porous media (Yortsos 1990; Philips 1991; Bedrikovetsky 1993; Araque-Martinez and Lake 1999, 2001; Rocha et al. 2001; Delshad and Pope 2003).

The main assumptions of the mathematical model for sulfate scaling and consequent formation damage are as follows:

- Irreversible chemical reaction between sulfate anions and cations of barium (strontium, calcium)
- Active-mass law for kinetics of the second-order chemical reaction
- Instantaneous deposition of the appearing salt without its transport through the rock
- Independence of reaction-rate constant on deposited concentration
- Volume conservation during chemical reaction for the system aqueous solution of two reagents and solid deposit
- Constant temperature
- Negligible reagent dispersion

We assume that chemical reaction between barium and sulfate is irreversible and obeys the second-order active-mass law (Fogler 1998; Yortsos 1990). This hypothesis is valid for short times, when the system state is far away from thermodynamic equilibrium between the deposited salt and its aqueous solution. Short times correspond to low deposited concentrations. Kinetics of dissolution of the solid deposit in water must be taken into account for the case of high deposited concentrations during long-time tests.

It is assumed that the reaction-rate constant is independent of the deposited concentration. The assumption is valid for low deposited concentrations.

An instant deposition of formed sulfate salt is also assumed: Kinetics of crystal growth and precipitation (Nancollas and Liu 1975; Nielsen 1959) is neglected, and no migration of salt crystals through the rock takes place (Allaga et al. 1992).

The system of governing equations for flow of a SW and FW mixture with chemical reaction between two species consists of mass balance equations for barium cations, sulfate anions, and deposited salt and also of modified Darcy's law accounting for

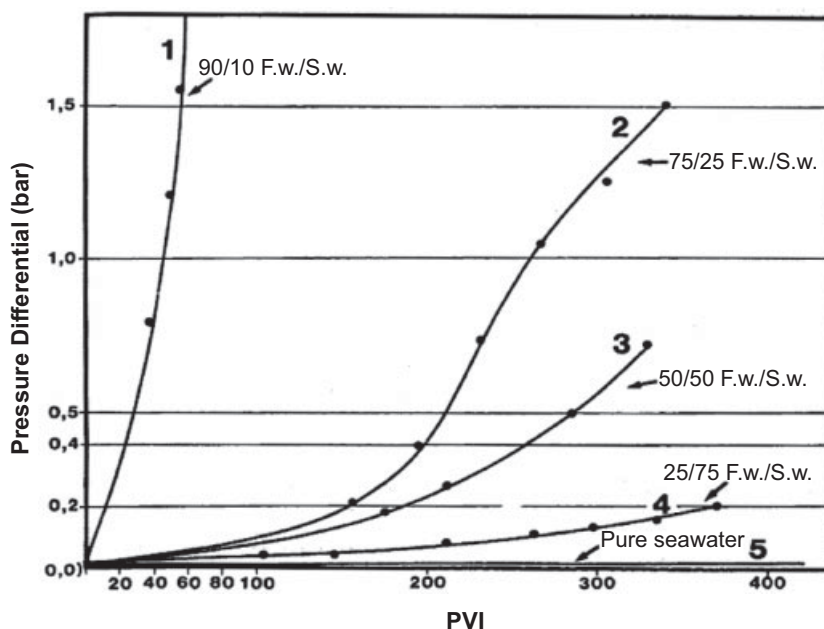


Fig. 4—Pressure drop during commingled injection in coreflood tests with different FW/SW ratios (Read and Ringen 1982).

permeability damage because of salt deposition (Araque-Martinez and Lake 1999; Philips 1991; Woods and Parker 2003):

$$\phi \frac{\partial c_{Ba}}{\partial t} + U \frac{\partial c_{Ba}}{\partial x} = -\lambda U c_{Ba} c_{SO_4} \dots (2)$$

$$\phi \frac{\partial c_{SO_4}}{\partial t} + U \frac{\partial c_{SO_4}}{\partial x} = -\lambda U c_{Ba} c_{SO_4} \dots (3)$$

$$\phi \frac{\rho_{BaSO_4}}{M_{BaSO_4}} \frac{\partial \sigma}{\partial t} = \lambda U c_{Ba} c_{SO_4} \dots (4)$$

$$U = -\frac{k_o}{\mu(1+\beta\sigma)} \frac{\partial p}{\partial x} \dots (5)$$

The chemical-reaction term in the right-hand side of Eqs. 2 and 3 contains the product of reagent concentrations [i.e., the active-mass law is fulfilled (Yortsos 1990; Fogler 1998)]. The term contains also flow velocity as a multiplier because the reaction-rate constant for barium sulfate reaction is proportional to velocity (Fogler 1998). The proportionality coefficient λ is called the kinetics coefficient.

The rock permeability decreases with increase of deposited concentration σ . The hyperbolic formula is assumed for dependence of permeability on deposited concentration (Pang and Sharma 1994):

$$k(\sigma) = \frac{k_o}{1+\beta\sigma} \dots (6)$$

where β is called the formation-damage coefficient.

It is assumed that the kinetics coefficient is independent of deposit and pressure. Therefore, Eqs. 2 and 3 separate from Eqs. 4 and 5. Solution of the system (Eqs. 2 and 3) determines the unknown ion concentrations. The deposited concentration is calculated from Eq. 4, provided that solution of the system (Eqs. 2 and 3) is already obtained. Afterwards, the pressure distribution is determined from Eq. 5.

Let us introduce dimensionless species concentrations and pressure (Eq. A-1) and also dimensionless coordinate, time and chemical kinetics number (Eq. A-2). It transforms the system of four governing equations (Eqs. 2 through 5) to its dimensionless form (Eqs. A-3 through A-6); see Appendix A.

The governing system (Eqs. A-3 through A-6) contains two dimensionless parameters: kinetics number ε_k and formation-damage coefficient β (Bedrikovetsky 2004).

The kinetics number is proportional to the kinetics coefficient that shows how fast the chemical reaction occurs. This parameter depends on temperature and ionic strength of the brine. It also depends on pore-space structure and mineralogical content of the

rock surface. The formation-damage coefficient depends on pore-space structure, pore-size distribution, coordination number, and tortuosity of the pore paths.

Mathematical models for sulfate scaling in porous media and related formulations of direct and inverse problems are similar to those for suspension filtration and consequent injectivity decline (Pang and Sharma 1994). Sulfate-scaling Eqs. 2 through 5 degenerate into deep-bed filtration models for the case in which sulfate concentration highly exceeds the barium (strontium) concentration, and sulfate-concentration variation can be ignored. So, Eq. 4 for the chemical reaction kinetics becomes equivalent to kinetics equation for particle capture in the model for suspension transport in porous media (Nabzar et al. 1996; Pang and Sharma 1997; Chauveteau et al. 1998; Al-Abduwani et al. 2005; Ali et al. 2005). Particle precipitation rate for both suspension transport and reactive flow is proportional to flow velocity. The proportionality coefficient λ (filtration coefficient) can be calculated from breakthrough concentration, while the formation-damage coefficient β , which is defined by Eq. 5, can be determined from the increase of pressure drop on the core during the flooding because of particle capture by the rock. Both coefficients can also be determined from pressure measurements (Alvarez et al. 2006a, 2006b). Knowledge of two coefficients λ and β along with numerical solution of the quasi-3D problem allows for reliable prediction of formation damage caused by drilling-fluid invasion into the formation (Bailey et al. 2000; Suryanarayana et al. 2007), forecast of injectivity decline in fractured injectors (Bachman and Settari 2003; Mojarad and Settari 2005), of produced-water reinjection injectivity (PWRI) impairment (Al-Abduwani et al. 2005; Ali et al. 2005), of fines migration and capture in low consolidated or heavy-oil fields (Zang and Dusseault 2004).

As well as the mathematical model for injectivity decline, 3D system of governing equations for oil and water flow with chemical reaction between metals and sulfate, describing sulfate scaling in production wells, contains the chemical kinetics and formation-damage coefficients, ε_k and β , respectively. Knowledge of these coefficients is necessary for the reliable prediction of production-well behavior during oilfield sulfate scaling. The obtained coefficients λ and β must be used in 3D modeling in different flow geometries for perforated, fractured, and horizontal wells (Bachman and Settari 2003; Mojarad and Settari 2005; Suryanarayana et al. 2007).

The following sections show that the values of the kinetics and formation-damage coefficients can be determined from quasisteady-state corefloods with commingled injection of SW and FW.

Analytical Model for Quasisteady-State Corefloods

Consider commingled flow of two reacting aqueous solutions in core with steady-state concentration profiles. Formulae for barium- and sulfate-ion concentration profiles are obtained in Appendix B:

$$C_{Ba} = \frac{(1-\alpha)}{e^{\varepsilon_k(1-\alpha)x_D} - \alpha} \dots (7)$$

$$C_{SO_4} = \frac{(1-\alpha)}{1 - \alpha e^{-\varepsilon_k(1-\alpha)x_D}} \dots (8)$$

The profiles (Eqs. 7 and 8) are steady state.

Fig. 5 shows concentration profiles for both reagents as calculated using the explicit formulae (Eqs. 7 and 8). The case corresponds to commingled coreflood carried out in work performed by Read and Ringen (1982) for ratios FW/SW=75:25 and 25:75 [i.e., for FW fraction in the overall flux $f=0.75$ and $f=0.25$, respectively (Curves 2 and 4 in Fig. 4)]. In both cases, sulfate concentration highly exceeds barium concentration (sulfate concentration profiles are located above the barium profiles in Fig. 5). Barium concentration in Case 2 exceeds that for Case 4 nine times, so the barium concentration in Case 2 declines faster than that for the Case 4 (Fig. 5). Sulfate concentrations in both cases highly exceed barium

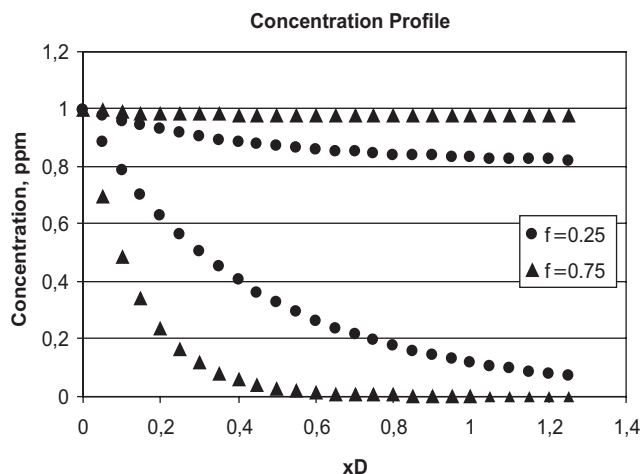


Fig. 5—Concentration profiles for barium and sulfate ions for the kinetics constant $\lambda = 4042 \text{ (Mm)}^{-1}$.

concentrations, so the difference between the sulfate concentrations in both cases is not as significant as that for barium.

The barium sulfate deposition profile is unsteady state. The salt deposited concentration is proportional to time; see Eq. B-9.

$$S = \varepsilon_k \left\{ \frac{(1-\alpha)^2}{e^{\varepsilon_k(1-\alpha)x_D} + \alpha[\alpha e^{-\varepsilon_k(1-\alpha)x_D} - 2]} \right\} t_D \quad \dots\dots\dots (9)$$

Two reagent concentrations (Eqs. 7 and 8) are steady state, explaining the proportionality (Eq. 9) between the deposited concentration S and dimensionless time t_D .

Let us introduce the dimensionless pressure drop as the reciprocal to injectivity index and call it the impedance:

$$J = \frac{\Delta p(t)}{\Delta p(t=0)} \quad \dots\dots\dots (10)$$

Since deposited concentration is proportional to t_D , impedance is also proportional to t_D (see Eq. B-12):

$$J = 1 + mt_D \quad \dots\dots\dots (11)$$

where the impedance slope m is

$$m = \frac{M_{\text{BaSO}_4}}{\rho_{\text{BaSO}_4}} \beta c_{\text{Ba}}^o \left\{ \frac{\alpha [e^{\varepsilon_k(\alpha-1)} - 1]}{\alpha e^{\varepsilon_k(\alpha-1)} - 1} \right\} \quad \dots\dots\dots (12)$$

The analytical model for sulfate scaling (Eqs. 7 through 12) allows determining the sulfate-scaling-damage parameters from coreflood tests on commingled flow of SW and injected water (Fig. 2).

Characterization of Sulfate-Scale-Damage System From Pressure Measurements

Here, we develop the method for determining the sulfate-scaling-damage parameters from pressure data during two sequential corefloods with commingled injection of SW and FW with two different FW/SW ratios.

Kinetics number ε_k can be calculated from the ratio of injected to breakthrough concentrations of barium (Figs. 2 and 3). The higher the kinetics coefficient is, the more intensive is the chemical reaction and the larger is the difference between inlet and outlet reagent concentrations. Therefore, the inverse problem for determination of the kinetics coefficient from the breakthrough curve is well posed (Alvarez et al. 2006a, 2006b). By fixing $x_D = 1$ in Eq. 7, one can calculate the kinetics number ε_k and, consequently, the kinetics coefficient λ .

Formation-damage coefficient β can be calculated from the pressure-drop increase during the commingled coreflood. The larger the formation-damage coefficient is, the higher is the permeability reduction and, consequently, the larger is the pressure-drop increase. Therefore, the inverse problem for determination of the formation-damage coefficient from pressure-drop history is also well posed (Alvarez et al. 2006a, 2006b).

Let us rewrite Eq. 12 in terms of FW fraction f in the total injected flux (SW fraction is equal to $1-f$):

$$m = \beta c_{\text{Ba}}^o f \frac{M_{\text{BaSO}_4}}{\rho_{\text{BaSO}_4}} \left\{ \frac{\left\{ \frac{e^{\varepsilon_k[f(\alpha+1)-1]} - 1}{\alpha \frac{f}{(1-f)} e^{\varepsilon_k[f(\alpha+1)-1]} - 1} \right\}}{\left\{ \frac{e^{\varepsilon_k[g(\alpha+1)-1]} - 1}{\alpha \frac{g}{(1-g)} e^{\varepsilon_k[g(\alpha+1)-1]} - 1} \right\}} \right\} \quad \dots\dots\dots (13)$$

The impedance growth coefficient m can be found from pressure-drop measurements (Eq. 10). If the kinetics number is already known from the breakthrough concentration, Eq. 13 allows for calculation of formation-damage coefficient β .

Pressure-drop measurements are simple, reliable, and require standard laboratory equipment. Concentration measurements are cumbersome and require more complex equipment. Therefore, it is attractive to develop a method for determination of scale-damage parameters from pressure measurements only.

Several corefloods with commingled injection of SW and FW with pressure-drop measurements have been performed by Read and Ringen (1982). Fig. 4 shows pressure-drop development during five corefloods. The details of the tests are described in the section "Analytical Model for Quasisteady-State Corefloods."

Assuming that the scaling-damage parameters are equal for two cores, let us calculate the parameters from the tests with different FW/SW ratios.

Consider Eq. 13 for two tests with two different fractions of formation water in the overall flux, f and g . These two equations form a system for two unknowns ε_k and β . Dividing Eq. 13 with fraction g by that with fraction f , we obtain one transcendental equation for unknown ε_k :

$$\frac{Mg \left\{ \frac{e^{\varepsilon_k[g(\alpha+1)-1]} - 1}{\alpha \frac{g}{(1-g)} e^{\varepsilon_k[g(\alpha+1)-1]} - 1} \right\}}{\alpha \frac{g}{(1-g)} e^{\varepsilon_k[g(\alpha+1)-1]} - 1} = \frac{f \left\{ \frac{e^{\varepsilon_k[f(\alpha+1)-1]} - 1}{\alpha \frac{f}{(1-f)} e^{\varepsilon_k[f(\alpha+1)-1]} - 1} \right\}}{\alpha \frac{f}{(1-f)} e^{\varepsilon_k[f(\alpha+1)-1]} - 1} \quad \dots\dots\dots (14)$$

where the constant M is equal to $M = \frac{m_f}{m_g}$.

The kinetics number ε_k is calculated numerically by solution of the transcendental equation (Eq. 14). Then the formation-damage coefficient is calculated explicitly from Eq. 13.

Results of Laboratory Data Treatment for Artificial Cores

In this section, the values of two sulfate-scaling-damage parameters are calculated from the pressure-drop data during commingled injections of incompatible waters with different FW/SW ratios, in artificial cores. The data of the laboratory study by Read and Ringen (1982) are used.

The FW/SW ratio in the fourth test is 1:3 (Fig. 4). Because the barium/sulfate concentration ratio $\alpha = 1/16$, the concentration ratio of sulfate to barium in the bulk injected liquid is 48. So, the reaction occurs under high sulfate excess; its rate is determined by barium concentration. Thus, the deposited concentration at the end of the test [370 pore volumes injected (PVI)] is relatively low if compared with three other tests, and it can be assumed that deposition does alter pore-space geometry and the reaction conditions (i.e., the kinetics coefficient λ is constant). Therefore, in accordance with Eq. 11, the fourth-test curve is almost linear.

In the third test, the FW/SW ratio is 1:1. The concentration ratio of sulfate to barium in the bulk liquid is 16 (i.e., three times lower than that in fourth test). Therefore, the deposited concentration in the third test at the end of flooding (330 PVI) is higher than that in the fourth test, and the impedance curve becomes nonlinear. We considered the linear growth in the third test only until the moment 200 PVI.

The nonlinear behavior of the curve $\Delta p(t_D)$ shows that some violations of the model assumptions happen after the moment of 200 PVI. Dissolution of the BaSO_4 solid salt in water is not accounted for in the model (Tests 2 through 5). Therefore, one of the ways around is the introduction of nonequilibrium solid/water-interface mass transfer into Eq. 4 for the deposition kinetics (Yortsos 1990; Bedrikovetsky 1993; Fogler 1998). Another explanation for disagreement between the laboratory nonlinear impedance curve and the modeling straight line (Eq. 11) is the change of the solid/water interface during the deposition, causing alteration of chemical-reaction kinetics (i.e., the kinetics number ε_k becomes S -dependent).

The FW/SW ratio in the second test is 3:1, and the concentration ratio α is 16:3. The pressure-drop curve exhibits nonlinearity because of large deposition and reaction-kinetics alteration. The linear development of impedance in this case was considered until the moment of 190 PVI.

Let us determine the λ and β values from Tests 3 and 4. Fig. 6a shows plots of the values of the left- and right-hand sides of Eq. 14 [functions $f(\varepsilon_k)$ and $g(\varepsilon_k)$, respectively] vs. unknown kinetics number ε_k . Two curves intersect in a single point, indicating the existence and uniqueness of the solution in the considered particular case. The obtained value $\varepsilon_k = 9.95$ can be seen clearly

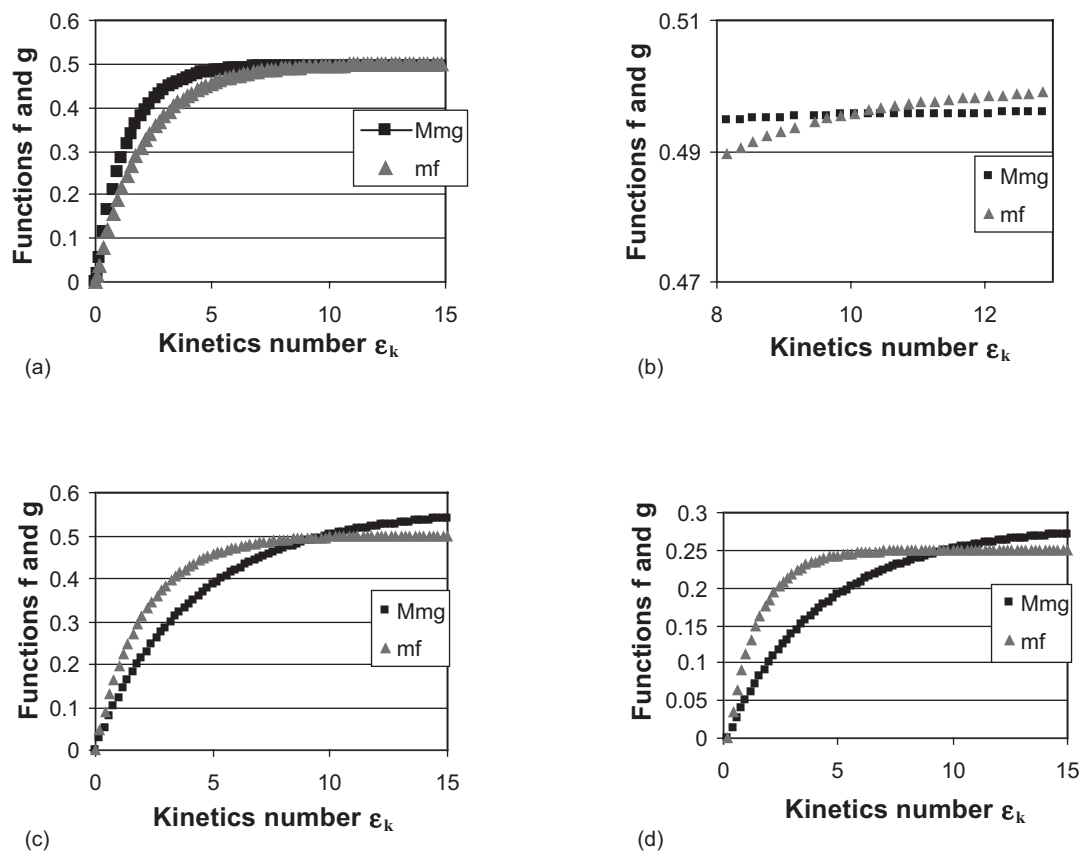


Fig. 6—Solution of the transcendental equation (Eq. 14) for determining the kinetics coefficient: (a) from the third and fourth tests; its zoom is shown in (b); (c) from the second and third tests, with $M=m_3/m_2$; (d) from the fourth and second tests, $M=m_4/m_2$.

in the zoom (Fig. 6b). The kinetics coefficient is calculated from a dimensionless expression (Eq. A-2) for kinetics number ε_k : $\lambda = 4146 \text{ (Mm)}^{-1}$. The formation-damage coefficient is determined from Eq. 13: $\beta = 28.4$.

The proposed method for determination of λ and β from core-floods with different ratios of injected seawater and formation water can be validated by independent treatment of the data from different tests couples. Let us determine the coefficients λ and β from Tests 2 and 3, and also from Tests 2 and 4, and compare the results. Fig. 6c shows plots of functions $f(\varepsilon_k)$ and $g(\varepsilon_k)$ (left- and right-hand sides of Eq. 14, respectively) for Tests 3 and 2. Fig. 6d shows plots of functions $f(\varepsilon_k)$ and $g(\varepsilon_k)$ for the pairs of Tests 4 and 2. In each case, the curves cross in a single point, so a solution of Eq. 14 exists and the solution is unique.

The results are presented in Table 1. As expected, the scaling-damage parameters are almost equal for the three cases.

Since the three tests have been performed in similar artificial cores, the conditions of chemical reaction are the same and the kinetics coefficients must also be the same. The formation-damage coefficient depends on pore-space structure and crystal size and must also be equal for the three tests. The agreement between three values of parameters as obtained from three different laboratory

tests (from three independent sources of information) validates the method proposed.

Results of Laboratory Data Treatment for Reservoir Cores

To apply the method of two water ratios to real reservoir cores, the commingled corefloods with different FW/injected-water ratios were performed in three Berea cores. The data of three tests with Berea Cores 2, 3, and 4 are shown in Table 2.

Figs. 7 and 8 present graphical solution of transcendental equation (Eq. 14) to determine the kinetics number. Calculation from two tests Berea 2 and 2-5 (Fig. 7) results in $\lambda = 371.24 \text{ (Mm)}^{-1}$, $\beta = 1584.63$. From the set of tests Berea 2 and 3-5 were obtained the following averaged data: $\lambda = 415.28 \text{ (Mm)}^{-1}$, $\beta = 1480.72$ (Fig. 8).

The solution stability in Figs. 7 and 8 is lower than that for artificial cores (Fig. 6). Small perturbation of measured data m_f and m_g may result in significant variation of intersection-point coordinates (root of Eq. 14). The stability of the method can be increased by stochastic regularization [i.e., by small stochastic Monte Carlo perturbations of raw data for pressure-drop measurements $\Delta p(t_i)$,

TABLE 1—KINETICS AND FORMATION-DAMAGE COEFFICIENTS AS OBTAINED FROM DIFFERENT PAIRS OF TESTS WITH DIFFERENT RATIOS FW TO SW				
Tests	Kinetic number ε_k	Kinetic coefficient λ , 1/mm	Formation damage coefficient, β	Constant M
2–3	9.54	3975	22.13	1.33
2–4	9.60	4000	27.90	2.64
3–4	9.95	4146	28.40	1.98
medium	9.70	4042	26.14	

TABLE 2—PARAMETERS OF COREFLOODS

Core	Permeability (md)	Porosity (%)	Length (m)	Diameter (m)	Rate (mL/min)	Injection time, min	Injection time, pvi	FW:SW
Berea 1	752.5	24.21	0.0661	0.0381	4	135+22	29.6+5	1:1 + 3:1
Berea 2	88.39	21.11	0.10212	0.03788	4	42	7	1:3
Berea 3	85.06	21.09	0.10135	0.03787	4	33	5.5	1:1
Berea 4	91.11	21.69	0.10229	0.03781	4	30	5	1:1

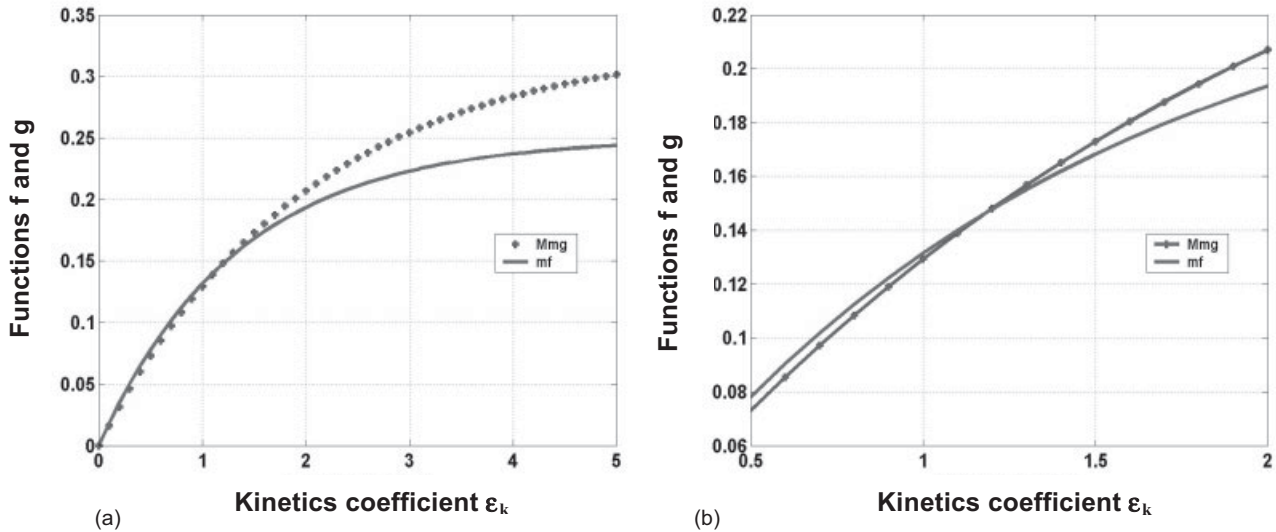


Fig. 7—Solution of the transcendental equation (Eq. 14) to determine the kinetics number from tests Berea 2 and 3: (a) graphical solution; (b) its zoom near the root of the equation.

$\Delta p(t_2) \dots$ and by averaging of m_f and m_g values as obtained from sequence realizations [see Tikhonov and Arsenin (1977)].

The results from Figs. 7 and 8 are different. It indicates the effect of porous media on sulfate formation damage (natural Berea cores are similar but not identical). The importance of porous-media microcharacteristics on sulfate scaling has been mentioned in several publications (Oddo and Tomson 1994; Rosario and Bezerra 2001; Gomes et al. 2002; Mackay 2002; Mackay and Graham 2002;

Mackay et al. 2003). Nevertheless, systematic study of the effects of factors such as permeability, porosity, tortuosity, and coordination number on the kinetics constant is not available in the literature.

The uncertainty caused by nonidentical natural reservoir rock samples can be decreased by using several similar cores taken from the same formation and by least-squares result treatment. Yet, the problems of sample representativity and the core choice criteria must be addressed in further research.

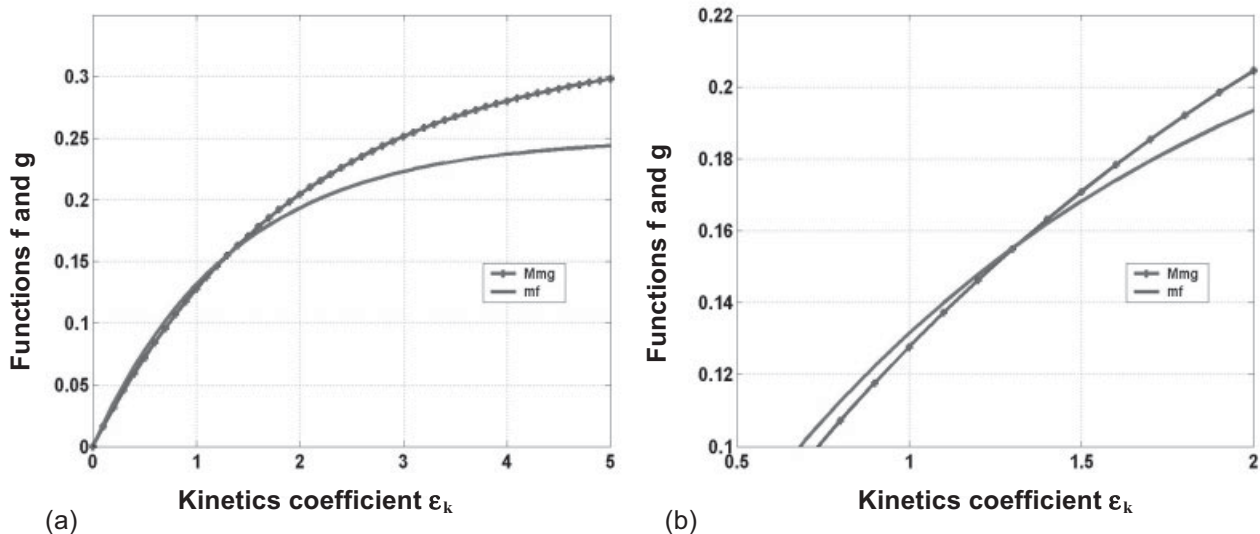


Fig. 8—Graphical solution of the transcendental equation (Eq. 14) to determine the kinetics number from tests Berea 2 and 4 (a); its zoom is shown in (b).

A Method of Two Sequential Injections in the Same Reservoir Core

This section contains the description of a method to determine two sulfate-scaling-damage coefficients from two sequential injections in the same reservoir core. The method consists of two commingled injections of water with different ratios of FW/injection water, with simultaneous pressure-drop measurement.

Deviation of the pressure-drop curve with intensive sulfate precipitation from the modeling results (Curve 1 in Fig. 4) indicates that the salt deposition changes matrix surface and conditions for further reaction and precipitation. Therefore, in order to keep the assumptions of Model 1-3 during the second flood, it is necessary to minimize sulfate precipitation during first injection. So, the only linear form of impedance $J(t_p)$ is established during the first injection, the system must be switched to the second flood.

As was mentioned above, sulfate scaling Model 2-5 is equivalent to that for deep-bed filtration in the case in which sulfate concentration is exceedingly higher than that of barium and can be considered to be constant. As in commingled coreflooding with SW and FW, both injectivity damage parameters λ and β can be determined from effluent particle concentration and pressure-drop evolution on the core. The additional information to substitute for complex and cumbersome breakthrough concentration measurements is the pressure-drop history on the first core section, which requires additional pressure measurement at some intermediate point of the core (Bedrikovetsky et al. 2001). For oilfield sulfate scaling, the corresponding additional information is obtained from commingled coreflood with two different ratios of FW/injected water.

The test was performed with core Berea 1. The test data are presented in Table 2. Fig. 9 shows the result of the solution of the transcendental equation (Eq. 14), abscissa of the intersection point of the two curves corresponds to the kinetics number ε_k . From the root $\varepsilon_k = 14.96$ was calculated the kinetics coefficient $\lambda = 7246.88 \text{ (Mm)}^{-1}$. Formation-damage coefficient $\beta = 45817.4$ was calculated from Eq. 13. The obtained values of sulfate-damage coefficients are in the common range of these parameters.

Fig. 10 shows graphical determination of the root on plane (β, λ) . Horizontal lines $\lambda = 5975 \text{ (Mm)}^{-1}$ and $\lambda = 8147 \text{ (Mm)}^{-1}$ correspond to measurement of effluent barium concentration ($c_1 = 0.32$

and $c_2 = 4.27 \text{ ppm}$, respectively) and calculation of the kinetics coefficient using 7. The kinetics-coefficient values obtained from effluent concentration and from pressure-drop measurements are different. We attribute the difference to the heterogeneity of the core, which results in inhomogeneous profiles of kinetics and formation-damage coefficients along the core.

Discussions

The analytical model for commingled flow of SW and FW shows that pressure drop on the core grows linearly with time only in the case of constant kinetics and formation-damage coefficients. The laboratory data also show that the linear dependence takes place only for the case of constant sulfate-scaling coefficients, which corresponds to low deposited concentrations. At high deposit concentrations, the laboratory tests exhibit nonlinear behavior of pressure drop. The proposed method for determination of scale-damage parameters from pressure measurements was validated successfully for “linear” periods of corefloods for three low-deposit tests in artificial cores. The method was shown to be invalid for the test with intensive deposition and nonlinear behavior of pressure drop.

Nonequilibrium dissolution of salt in water and dependence of kinetics coefficient on deposit concentration can be accounted for in the mathematical model in order to treat nonlinear impedance curves from commingled corefloods by SW and FW.

Some tests expose a small angle between lines $f(\varepsilon_k)$ and $g(\varepsilon_k)$ near the intersection point, resulting in instability of the root of Eq. 14 (Figs. 6a, 7, and 8). The stability can be increased by modeling the errors in measurements (i.e., by small stochastic perturbation of measured pressure-drop values and by averaging the slopes m_f and m_g as obtained from different realizations).

The uncertainty caused by non-identical properties of similar rock samples limits the application of the method for natural reservoir cores. The uncertainty can be reduced by the use of several cores, although the required number of cores for determining the values of chemical kinetics and formation-damage coefficients is two. Yet, the problems of sample selection criteria and of rock sample representativity must be addressed after accumulation of sufficient data on application of the proposed method for reservoir core samples.

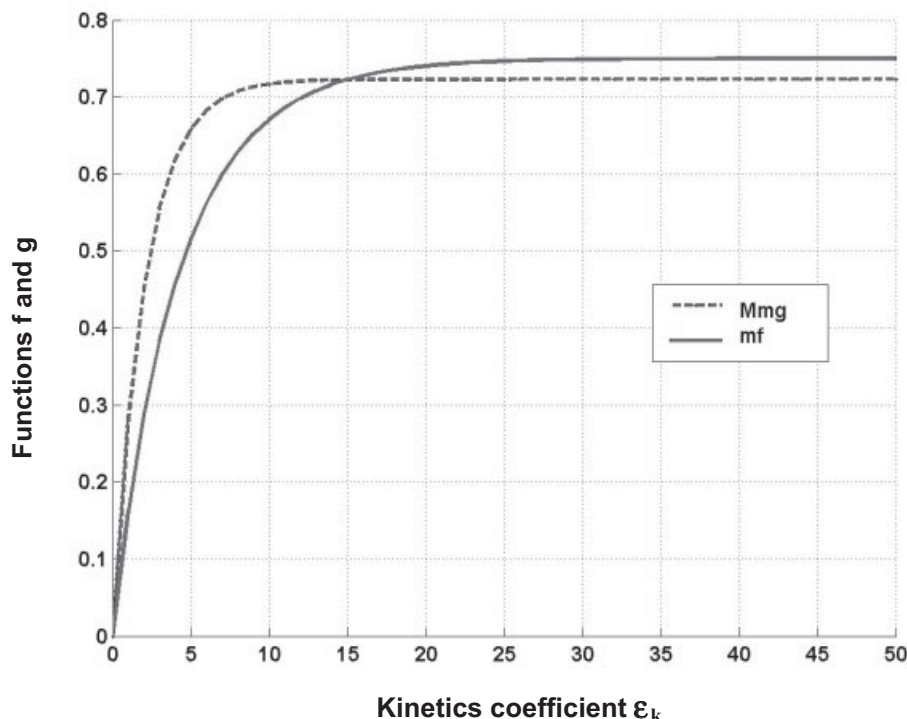


Fig. 9—Graphical solution of the transcendental equation (Eq. 14) to determine the kinetics number from test Berea 1.

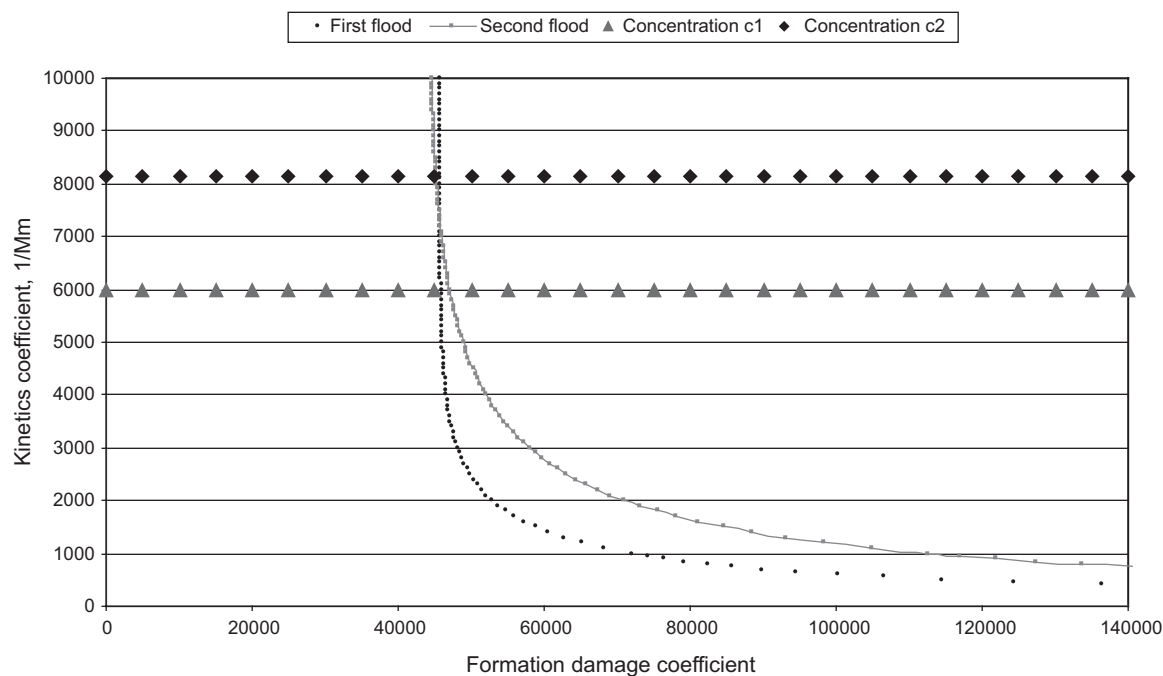


Fig. 10—Graphical determination of the root on plane (λ, β) from test Berea 1 and its comparison with that obtained from breakthrough concentrations.

The proposed method is similar to that for determination of two injectivity-damage parameters for rock clogging by captured particles from pressure-drop measurements during coreflooding. Currently, this method is used on offshore platforms and on site in onshore fields, avoiding the transport of waters and cores to laboratory, storage problems, etc. [see Vaz et al. (2009)]. The proposed method must be developed and tested further for use at on-site oilfield conditions.

Conclusions

Treatment of laboratory data on two sequential commingled core-floods by two incompatible waters with different ratios of FW/SW in the same core allows us to conclude the following:

- Two sulfate-scaling-damage parameters—kinetics and formation-damage coefficients—can be determined from two commingled core-floods with two different FW/SW ratios in a single core;
- Stability of the method is significantly higher for artificial cores than for natural reservoir cores.

Nomenclature

- c_{Ba} = Ba^{2+} molar concentration in aqueous solution, M
 c_{SO_4} = SO_4^{2-} molar concentration in aqueous solution, M
 C_{Ba} = dimensionless Ba^{2+} concentration
 C_{SO_4} = dimensionless SO_4^{2-} concentration
 f, g = FW fraction in the total flux
 J = dimensionless impedance
 k = permeability, d
 k_o = initial permeability, d
 L = core length, m
 m = slope of the impedance straight line vs. t_D
 M_{BaSO_4} = molecular weight for barium sulfate in gmol/L (equals Kg mol/m³)
 p = pressure, Pa
 P = dimensionless pressure
 S = dimensionless $BaSO_4$ concentration
 t = time, seconds
 t_D = dimensionless time, PVI
 U = flow velocity, m/s
 x = linear coordinate
 x_D = dimensionless linear coordinate
 α = ratio between injected concentrations of Ba^{2+} and SO_4^{2-}
 β = Formation-damage coefficient

- ε_k = dimensionless chemical kinetics number
 λ = kinetics coefficient, (Mxm)⁻¹ (second-order reaction)
 μ = viscosity, kg/(m·s)
 ρ_{BaSO_4} = density of the barite, kg/m³
 σ = $BaSO_4$ molar concentration in solid deposit, M
 ϕ = porosity

Acknowledgments

Many thanks are owed to Petrobras for generous sponsorship of the project. The authors gratefully acknowledge Francisca Rosario (Petrobras/Cenpes) for support and encouragement during many years of cooperation. E. Mackay (Heriot Watt University) is gratefully acknowledged for improvement of the readability of the paper.

Special thanks are due to Y. Yortsos (University of Southern California) and J.K. Ringen (Statoil, Norway) for numerous fruitful discussions.

References

- Al-Abduwani, F.A.H., Shirzadi, A., van den Broek, W.M.G.T., and Currie, P.K. 2005. Formation Damage vs. Solid Particles Deposition Profile During Laboratory-Simulated Produced-Water Reinjection. *SPE J.* **10** (2): 138–151. SPE-82235-PA. doi: 10.2118/82235-PA.
- Ali, M.A.J., Currie, P.K., and Salman, M.J. 2005. Measurement of the Particle Deposition Profile in Deep-Bed Filtration During Produced Water Re-Injection. Paper SPE 93056 presented at the SPE Middle East Oil and Gas Show and Conference, Bahrain, 12–15 March. doi: 10.2118/93056-MS.
- Alliaga, D.A., Wu, G., Sharma, M.M., and Lake, L.W. 1992. Barium and Calcium Sulphate Precipitation and Migration Inside Sandpacks. *SPE Form Eval* **7** (1): 79–86; *Trans.*, AIME, **293**. SPE-19765-PA. doi: 10.2118/19765-PA.
- Alvarez, A.C., Bedrikovetsky, P.G., Hime, G., Marchesin, A.O., Marchesin, D., and Rodríguez, J.R. 2006a. A fast inverse solver for the filtration function for flow of water with particles in porous media. *Inverse Problems* **22**: 69–88. doi: 10.1088/0266-5611/22/1/005.
- Alvarez, A.C., Hime, G., Marchesin, D., and Bedrikovetsky, P.G. 2006b. The inverse problem of determining the filtration function and permeability reduction in flow of water with particles in porous media. *Transport in Porous Media* **70** (1): 43–62. doi: 10.1007/s11242-006-9082-3.
- Araque-Martinez, A.N. and Lake, L.W. 1999. A Simplified Approach to Geochemical Modeling and its Effect on Well Impairment. Paper SPE 56678 presented at the SPE Annual Technical Conference and Exhibition, Houston, 3–6 October. doi: 10.2118/56678-MS.

- Araque-Martinez, A.N. and Lake, L.W. 2001. A Simplified Approach to Geochemical Modeling and its Effect on Mineral Precipitation. *SPE J.* **6** (1): 98–107. SPE-69743-PA. doi: 10.2118/69743-PA.
- Bachman, R.C., Harding, T.G., Settari, A., and Walters, D.A. 2003. Coupled Simulation of Reservoir Flow, Geomechanics, and Formation Plugging With Application to High-Rate Produced Water Reinjection. Paper SPE 79695 presented at the SPE Reservoir Symposium, Houston, 3–5 February. doi: 10.2118/79695-MS.
- Bailey, L., Boek, E.S., Jacques, S.D.M., Boassen, T., Selle, O.M., Argillier, J.F., and Longeron, D.G. 2000. Particulate Invasion From Drilling Fluids. *SPE J.* **5** (4): 412–419. SPE-67853-PA. doi: 10.2118/67853-PA.
- Bedrikovetsky, P., Marotti, M., Lima Neto, I.A., and Carageorgos, T. 2007. Characterization of Sulphate Scale Damage System from Pressure Measurements. Paper SPE 107884 presented at the SPE Latin American & Caribbean Petroleum Engineering Conference, Buenos Aires, 15–18 April. doi: 10.2118/107884-MS.
- Bedrikovetsky, P.G. 1993. *Mathematical Theory of Oil and Gas Recovery: With Applications to ex-USSR Oil and Gas Fields*, Vol. 4, ed. G. Rowan, trans. R. Loshak. Dordrecht, The Netherlands: Petroleum Engineering and Development Studies, Kluwer Academic Publishers.
- Bedrikovetsky, P.G., Marchesin, D., Checaira, F., Serra, A.L., and Resende, E. 2001. Characterization of Deep Bed Filtration System from Laboratory Pressure Drop Measurements. *J. Pet. Sci. Eng.* **64** (3): 167–177.
- Bedrikovetsky, P.G., Lopes, R.P.J., Gladstone, P.M., Rosario, F.F., Bezerra, M.C., and Lima, E.A. 2004. Barium Sulphate Oilfield Scaling: Mathematical and Laboratory Modelling. Paper SPE 87457 presented at the SPE International Symposium on Oilfield Scale, Aberdeen, 26–27 May. doi: 10.2118/87457-MS.
- Bethke, C.M. 1996. *Geochemical Reaction Modeling*. Buckingham, UK: Oxford University Press.
- Chauveteau, G., Nabzar, L., and Coste, J.-P. 1998. Physics and Modeling of Permeability Damage Induced by Particle Deposition. Paper SPE 39463 presented at the SPE Formation Damage Control Conference, Lafayette, Louisiana, USA, 18–19 February. doi: 10.2118/39463-MS.
- Civan, F. 2007. *Reservoir Formation Damage: Fundamentals, Modeling, Assessment, and Mitigation*, second edition, 742. Burlington, Massachusetts, USA: Gulf Professional Publishing/Elsevier.
- Delshad, M. and Pope, G.A. 2003. Effect of Dispersion on Transport and Precipitation of Barium and Sulfate in Oil Reservoirs. Paper presented at the International Symposium on Oilfield Chemistry, Houston, 5–7 February. doi: 10.2118/80253-MS.
- Fogler, H.S. 1998. *Elements of Chemical Reaction Engineering*, third edition. Upper Saddle River, New Jersey, USA: Prentice-Hall International Series in the Physical and Chemical Engineering Sciences, Prentice Hall PTR.
- Gomes, J., Bezerra, M.C., Daher, J.S., and Rosario, F.F. 2002. The Impact of Mineral Scale Formation on Deep Water Fields: A Campos Basin Overview. Prepared for presentation at the International Symposium on Oilfield Scale, Aberdeen, 30–31 January.
- Kechagia, P.E., Tsimplanogiannis, I.N., Yortsos, Y.C., and Lichtner, P.C. 2002. On the upscaling of reaction-transport processes in porous media with fast or finite kinetics. *Chemical Engineering Science* **57** (13): 2565–2577. doi: 10.1016/S0009-2509(02)00124-0.
- Lopes, R.P.J. 2002. Barium Sulphate Kinetics of Precipitation in Porous Media: Mathematical and Laboratory Modeling, in Portuguese, MSc thesis, North Fluminense State University, Macaé, Rio de Janeiro.
- Mackay, E.J. 2002. Modeling of In-Situ Scale Deposition: The Impact of Reservoir and Well Geometries and Kinetics Reaction Rates. Paper SPE 74683 presented at the International Symposium on Oilfield Scale, Aberdeen, 30–31 January. doi: 10.2118/74683-MS.
- Mackay, E.J. and Graham, G.M. 2002. The Use of Flow Models in Assessing the Risk of Scale Damage. Paper SPE 80252 presented at the International Symposium on Oilfield Chemistry, Houston, 5–7 February. doi: 10.2118/80252-MS.
- Mackay, E.J., Jordan, M.M., and Torabi, F. 2003. Predicting Brine Mixing Deep within the Reservoir, and the Impact on Scale Control in Marginal and Deepwater Developments. *SPE Prod & Fac* **18** (3): 210–220. SPE-85104-PA. doi: 10.2118/85104-PA.
- Mackay, E.J. and Jordan, M.M. 2005. Impact of Brine Flow and Mixing in the Reservoir on Scale Control Risk Assessment and Subsurface Treatment Options: Case Histories. *J. Energy Resour. Technol.* **127** (3): 201–213. doi: 10.1115/1.1944029.
- Mojarad, R.S. and Settari, A. 2005. Multidimensional Velocity-Based Model of Formation Permeability Damage: Validation, Damage Characterization, and Field Application. Paper SPE 97169 presented at the SPE Annual Technical Conference and Exhibition, Dallas, 9–12 October. doi: 10.2118/97169-MS.
- Nabzar, L., Chauveteau, G., and Roque, C. 1996. A New Model for Formation Damage by Particle Retention. Paper SPE 31119 presented at the SPE Formation Damage Control Conference, Lafayette, Louisiana, USA, 14–15 February. doi: 10.2118/31119-MS.
- Nancollas, G. and Liu, T. 1975. Crystal Growth and Dissolution of Barium Sulfate. *SPE J.* **15** (6): 509–516; *Trans., AIME*, **259**. SPE-5300-PA. doi: 10.2118/5300-PA.
- Nielsen, A.E. 1959. The Kinetics of Crystal Growth in Barium Sulphate Precipitation. II. Temperature Dependence and Mechanism. *Acta Chemical Scandinavica* **13**: 784–802. doi: 10.3891/acta.chem.scand.13-0784.
- Oddo, J.E. and Tomson, M.B. 1994. Why Scale Forms and How to Predict It. *SPE Prod & Fac* **9** (1): 47–54. SPE-21710-PA. doi: 10.2118/21710-PA.
- Pang, S. and Sharma, M.M. 1997. A Model for Predicting Injectivity Decline in Water-Injection Wells. *SPE Form Eval* **12** (3): 194–201. SPE-28489-PA. doi: 10.2118/28489-PA.
- Philips, O.M. 1991. *Flow and Reactions in Porous Media*. Cambridge University Press.
- Read, P.A. and Ringen, J.K. 1982. The Use of Laboratory Tests to Evaluate Scaling Problems During Water Injection. Paper SPE 10593 presented at the SPE Oilfield and Geothermal Chemistry Symposium, Dallas, 25–27 January. doi: 10.2118/10593-MS.
- Rocha, A.A., Frydman, M., da Fontoura, S.A.B., Rosario, F.F., and Bezerra, M.C.M. 2001. Numerical Modeling of Salt Precipitation during Produced Water Reinjection. Paper SPE 68336 presented at the International Symposium on Oilfield Scale, Aberdeen, 30–31 January. doi: 10.2118/68336-MS.
- Rosario, F.F. and Bezerra, M.C. 2001. Scale Potential of a Deep Water Field—Water Characterization and Scaling Assessment. Paper SPE 68332 presented at the International Symposium on Oilfield Scale, Aberdeen, 30–31 January. doi: 10.2118/68332-MS.
- Sorbie, K.S. and MacKay, E.J. 2000. Mixing of injected, connate and aquifer brines in waterflooding and its relevance to oilfield scaling. *J. Pet. Sci. Eng.* **27** (1–2): 85–106. doi: 10.1016/S0920-4105(00)00050-4.
- Suryanarayana, P.V.R., Wu, Z., and Ramalho, J. 2007. Dynamic Modeling of Invasion Damage and Impact on Production in Horizontal Wells. *SPE Res Eval & Eng* **10** (4): 348–358. SPE-95861-PA. doi: 10.2118/95861-PA.
- Tikhonov, A.N. and Arsenin, V.Y. 1977. *Solutions of Ill-Posed Problems*. New York City: V.H. Winston and Sons.
- Todd, A.C. and Yuan, M.D. 1992. Barium and Strontium Sulphate Solid-Solution Scale Formation at Elevated Temperatures. *SPE Prod Eng* **7** (1): 85–92. SPE-19762-PA. doi: 10.2118/19762-PA.
- Vaz, A.S.L. Jr., Bedrikovetsky, P., Furtado, C., and de Souza, A.L.S. *In press*. Well Injectivity Decline for Non-linear Filtration of Injected Suspension: Semi-analytical model. *Journal of Energy Resources Technology* (accepted June 2009).
- Wat, R.M.S., Sorbie, K.S., Todd, A.C., Ping, C., and Ping, J. 1992. Kinetics of BaSO₄ Crystal Growth and Effect in Formation Damage. Paper SPE 23814 presented at the SPE Formation Damage Control Symposium, Lafayette, Louisiana, USA, 26–27 February. doi: 10.2118/23814-MS.
- Woods, A.W. and Parker, G. 2003. Barium Sulphate Precipitation in Porous Rock Through Dispersive Mixing. Paper SPE 80401 presented at the International Symposium on Oilfield Scale, Aberdeen, 29–30 January. doi: 10.2118/80401-MS.
- Yortsos, Y.C. 1990. Reaction and transport in porous media. Lecture notes on modeling and application of transport phenomena in porous media. VKI Lecture Series, von Karman Institut, Brussels, Belgium.
- Yuan, M.D. and Todd, A.C. 1991. Prediction of Sulphate Scaling Tendency in Oilfield Operations. *SPE Prod Eng* **6** (1): 63–72. SPE-18484-PA. doi: 10.2118/18484-PA.
- Zang, L. and Dusseault, M.B. 2004. Sand-Production Simulation in Heavy-Oil Reservoirs. *SPE Res Eval & Eng* **7** (6): 399–407. SPE-89037-PA. doi: 10.2118/89037-PA.

Appendix A—Dimensionless Equations for 1D Reactive Transport in Rocks

Let us introduce dimensionless parameters and coordinates

$$C_{Ba} = \frac{c_{Ba}}{c_{Ba}^o}, C_{SO_4} = \frac{c_{SO_4}}{c_{SO_4}^o}, S = \frac{\rho_{BaSO_4}}{M_{BaSO_4}} \frac{\sigma}{c_{Ba}^o}, P = \frac{k_o p}{U \mu L} \dots \dots \dots (A-1)$$

$$x_D = \frac{x}{L}, t_D = \frac{Ut}{\phi L}, \varepsilon_k = \lambda L c_{SO_4}^o, \alpha = \frac{c_{Ba}^o}{c_{SO_4}^o} \dots \dots \dots (A-2)$$

into the governing system of equations (Eqs. 2 through 5) for 1D reactive transport in porous media. We obtain the following system in dimensionless form (Bedrikovetsky et al. 2004, 2007):

$$\frac{\partial C_{Ba}}{\partial t_D} + \frac{\partial C_{Ba}}{\partial x_D} = -\varepsilon_k C_{Ba} C_{SO_4}, \dots (A-3)$$

$$\frac{\partial C_{SO_4}}{\partial t_D} + \frac{\partial C_{SO_4}}{\partial x_D} = -\alpha \varepsilon_k C_{Ba} C_{SO_4}, \alpha = \frac{C_{Ba}^o}{C_{SO_4}^o}, \dots (A-4)$$

$$\frac{\partial S}{\partial T} = \varepsilon_k C_{Ba} C_{SO_4}, \dots (A-5)$$

$$1 = -\frac{1}{1 + \beta \frac{M_{BaSO_4}}{\rho_{BaSO_4}} c_{Ba}^o S} \frac{\partial P}{\partial X}, \dots (A-6)$$

The system of four equations (Eqs. A-3 through A-6) determined four dimensionless unknowns: C_{Ba} , C_{SO_4} , S , and P . Eqs. A-3 and A-4 do not contain variables S and P , and, therefore, they separate from Eqs. A-5 and A-6. Eq. A-5 is independent of pressure P and separates from Eq. A-6. Therefore, the order of solution of the system (Eqs. A-3 through A-6) is as follows: First one solves system (Eqs. A-3 and A-4) and determines barium- and sulfate-ion concentrations; then, deposited salt concentration is determined from Eq. A-5 and, afterward, pressure P is calculated from Eq. A-6.

Appendix B—Derivation of Exact Solution for Commingled Injection of Incompatible Waters

Consider steady-state distributions of both ions. In this case, Eqs. A-3 and A-4 become a system of two ordinary-differential equations:

$$\frac{dC_{Ba}}{dx_D} = -\varepsilon_k C_{Ba} C_{SO_4}, \dots (B-1)$$

$$\frac{dC_{SO_4}}{dx_D} = -\alpha \varepsilon_k C_{Ba} C_{SO_4}, \dots (B-2)$$

Both reagent concentrations are fixed at the core inlet during the injection, providing boundary conditions for the system (Eq. B-1 and B-2):

$$x_D = 0: C_{Ba} = C_{SO_4} = 1. \dots (B-3)$$

Multiply Eq. B-1 by α and subtract it from Eq. B-2:

$$\frac{d(C_{SO_4} - \alpha C_{Ba})}{dx_D} = 0. \dots (B-4)$$

Integration in x_D results in the first integral for the system of two ordinary-differential equations (Eqs. B-1 and B-2). The constant value of $C_{SO_4} - \alpha C_{Ba}$ can be found from the inlet boundary condition (Eq. B-3):

$$C_{SO_4} - \alpha C_{Ba} = 1 - \alpha. \dots (B-5)$$

Expressing sulfate concentration from Eq. B-5 and substituting it into Eq. B-2, we obtain a first-order ordinary-differential equation

$$\frac{dC_{Ba}}{dx_D} = -\varepsilon_k C_{Ba} (\alpha C_{Ba} + 1 - \alpha). \dots (B-6)$$

It can be solved by separation of variables. Accounting for boundary conditions (Eq. B-3), we obtain the solution barium concentration profile:

$$C_{Ba} = \frac{(1 - \alpha)}{e^{\varepsilon_k (1 - \alpha) x_D} - \alpha}. \dots (B-7)$$

Substitution of Eq. B-7 into Eq. B-5 results in the sulfate-ion profile:

$$C_{SO_4} = \frac{(1 - \alpha)}{1 - \alpha e^{-\varepsilon_k (1 - \alpha) x_D}}. \dots (B-8)$$

Substituting Eqs. B-7 and B-8 into the equation for deposition rate (Eq. A-5) and integrating in t_D , we obtain the deposit distribution $S(x_D, t_D)$:

$$S = \varepsilon_k \left\{ \frac{(1 - \alpha)^2}{e^{\varepsilon_k (1 - \alpha) x_D} + \alpha [ae^{-\varepsilon_k (1 - \alpha) x_D} - 2]} \right\} t_D. \dots (B-9)$$

The two reagent concentrations are steady state, so deposited concentration is proportional to time t_D (Eq. B-9).

Let us introduce the dimensionless pressure drop as a reciprocal to injectivity index and call it the impedance:

$$J = \frac{\Delta p(t)}{U(t)} \frac{U(t=0)}{\Delta p(t=0)}. \dots (B-10)$$

Expressing pressure gradient from Eq. A-6 and integrating in x_D , we obtain the expression for impedance:

$$\Delta P = \int_0^1 -\frac{\partial P}{\partial X} dx_D = \int_0^1 \left(1 + \frac{M_{BaSO_4}}{\rho_{BaSO_4}} \beta \varepsilon_k C_{Ba}^o S \right) dx_D$$

Integrating the total yields

$$\Delta P = 1 + \frac{M_{BaSO_4}}{\rho_{BaSO_4}} \beta \varepsilon_k C_{Ba}^o \int_0^1 S(x_D, t_D) dx_D. \dots (B-11)$$

Performing integration in Eq. B-11 and accounting for the definition equation (Eq. B-10), we obtain the following formula for impedance:

$$J = 1 + \frac{M_{BaSO_4}}{\rho_{BaSO_4}} \beta C_{Ba}^o \left\{ \frac{\alpha [e^{\varepsilon_k (\alpha - 1)} - 1]}{\alpha e^{\varepsilon_k (\alpha - 1)} - 1} \right\} t_D. \dots (B-12)$$

SI Metric Conversion Factors

atm × 1.013 250*	E+05 = Pa
bar × 1.0*	E+05 = Pa
cp × 1.0*	E-03 = Pa·s
°F (°F×32)/1.8	= °C
ft × 3.048*	E-01 = m
knot × 5.144 444	E-01 = m/s

*Conversion factor is exact.

Themis Carageorgos is a research fellow at the Australian School of Petroleum at the U. of Adelaide. She holds a BSc degree in chemical engineering from the Fluminense Federal University (Brazil) and a PhD degree in hydrometallurgy from Imperial College of Science and Technology (U. of London). During 2000–2007, Carageorgos was an associated professor in petroleum engineering department at the State North Fluminense U. (Brazil). Her research interests lay in laboratory studies of flow in porous media and in minerals processing. **Marcelle Pinto Marotti** is a petroleum engineer at Petrobras (Brazil). She holds a BSc degree in mechanic engineering from the State U. of Rio de Janeiro and an MSc degree in reservoir engineering from North Fluminense State U. of Rio de Janeiro. Marotti's research interests lay in formation damage and reservoir modeling. **Pavel Bedrikovetsky** is a professor in petroleum engineering at the Australian School of Petroleum at the U. of Adelaide. His research covers formation damage, EOR, and nonlinear mathematical physics. Bedrikovetsky holds an MSc degree in applied mathematics, a PhD degree in fluid mechanics and a DSc degree in reservoir engineering from Moscow Gubkin Oil-Gas U. In 1991–1994, he was a visiting professor at Delft University of Technology and at Imperial College of Science and Technology. Since then, Bedrikovetsky has been a Petrobras senior staff consultant and also has done consulting for BP, BHP Total, Shell, Santos, and Statoil. He served as Section Chairman, short course instructor, key speaker and Steering Committee member at several SPE Conferences and ATW and as an 2008–2009 SPE Distinguished Lecturer.